Performance evaluation of transcritical CO_2 desiccant heat pumps for electric vehicles

Performance evaluation of transcritical CO_2 desiccant heat pumps for electric vehicles

H Wang[1,2], Y Song[2], F Cao[2], E Rossi di Schio[1], P Valdiserri[1]

[1] Department of Industrial Engineering, University of Bologna, Bologna, Italy
[2] School of Energy and Power Engineering, Xi'an Jiaotong University, Xi'an 710049, China
paolo.valdiserri@unibo.it; fcao@mail.xjtu.edu.cn

Abstract. Transcritical CO2 heat pump systems are eco-friendly and have excellent heating performance, which makes them suitable for electric vehicles. The recirculation mode can save energy but requires a dehumidification function to ensure driving safety. Therefore, this paper proposes a transcritical CO2 desiccant heat pump, which differs from the typical transcritical CO2 heat pump system by incorporating an indoor evaporator and a full-pass throttle valve. The flow area of the full-pass throttle valve can be adjusted to obtain the appropriate dehumidification rate. In addition, this study suggested using the desiccant heat pump coefficient of performance (DHCOP) to evaluate the overall energy efficiency of the heat pump system. We have investigated the dehumidification rate and optimal discharge pressure under different operating conditions. The results show that even under the harsh operating conditions at -10 °C, the HDCOP of the transcritical CO2 desiccant heat pump can still exceed 2.1, and reach 3.12 at a moderate condition of Ta=5 °C. The transcritical CO2 heat pump desiccant system demonstrates significant energy-saving potential.

1. Introduction

Electric vehicles (EVs) have emerged as a prominent solution to address environmental issues, such as greenhouse gas emissions and fossil fuel depletion [1]. However, EVs lack the waste heat generated by internal combustion engines and need additional heating load from Positive Temperature Coefficient (PTC) heaters, which significantly reduces driving range [2-3]. Therefore, researchers have proposed heat pump technology as an effective alternative to PTC heaters [4]. Generally, a fresh air heating mode is employed in winter to prevent windshield fogging, which introduces a significant heat load, accounting for over 70% of the total heat load [5]. Hence, reducing the ventilation load is a reasonable approach to save energy. In the recirculation mode, conditioning the indoor air to the desired state for thermal comfort can significantly reduce the ventilation load [6]. Zhang et al. [5] analyzed the climate control load of heat pump systems and concluded that the recirculation mode could save up to 48% of energy compared to the fresh air mode. However, the recirculation mode requires an additional dehumidification process to remove the moisture emitted by occupants and ensure driving safety [7]. To prevent windshield fogging, it is necessary to dehumidify the cabin air to a low humidity state, i.e., the dew point of the cabin air should be lower than the window's inner surface temperature. Li et al. [8] proposed fogging criteria to determine the relative humidity of cabin air. The results indicate that the relative humidity of the cabin air needs to be maintained at a low level, especially at low ambient

temperatures. For example, at an ambient temperature of -20 °C, the relative humidity should not exceed 9%. Therefore, even in dry winter conditions, the dehumidification function of the heat pump remains crucial for energy efficiency and driving safety. R134a, the most commonly used working fluid in heat pumps, has limited heating capacity in winter, especially at low ambient temperatures, due to the extremely low suction density leading to a decrease in heating capacity [9-10]. Thus, it is challenging for R134a heat pumps to meet the air reheating process after dehumidification. However, transcritical CO2 heat pump systems are eco-friendly and have excellent heating performance, which makes them highly suitable for EVs [11-13].

Few studies have been conducted on the dehumidification performance of transcritical CO2 heat pump systems in EVs. In this work, the authors establish a high-fidelity transcritical CO2 dehumidification heat pump system and propose a reasonable control scheme to reveal its optimal operational performance and dehumidification rate under operating conditions ranging from -10 ℃ to 5 ℃.

2. System description and modeling details

2.1. System description

Figure 1 displays the schematic diagram of a transcritical CO_2 desiccant heat pump system. Unlike traditional heat pump systems, the desiccant heat pump system incorporates an indoor evaporator and an all-through-throttle valve (throttle valve 2). In heating mode, throttle valve 2 is fully open, and the indoor evaporator is used as a gas cooler. In dehumidification mode, throttle valve 2 is in a throttling state, and the indoor evaporator is used as an evaporator. At this time, the high-humidity air is first cooled and dehumidified by the indoor evaporator and then heated to the desired temperature by the high-temperature CO_2 fluid in the indoor gas cooler. In dehumidification mode, the lgP-h diagram of the transcritical CO_2 fluid and the psychrometric chart diagram of air are shown in Figure 2. This paper exclusively investigates the recirculation mode.

In particular, this paper uses three PI controllers to achieve the desired dehumidification and heating capacity of the system:

(1) It Controls the compressor speed to achieve the desired supply air temperature of 42 ℃;
(2) It Controls the throttle valve 1 to achieve the desired discharge pressure;
(3) It Controls the throttle valve 2 to achieve the desired indoor evaporator pressure.

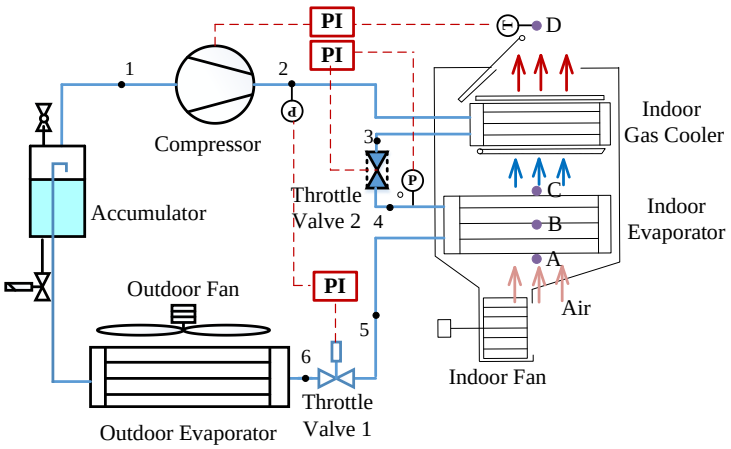

Figure 1. The schematic diagram of a transcritical CO_2 desiccant heat pump system.

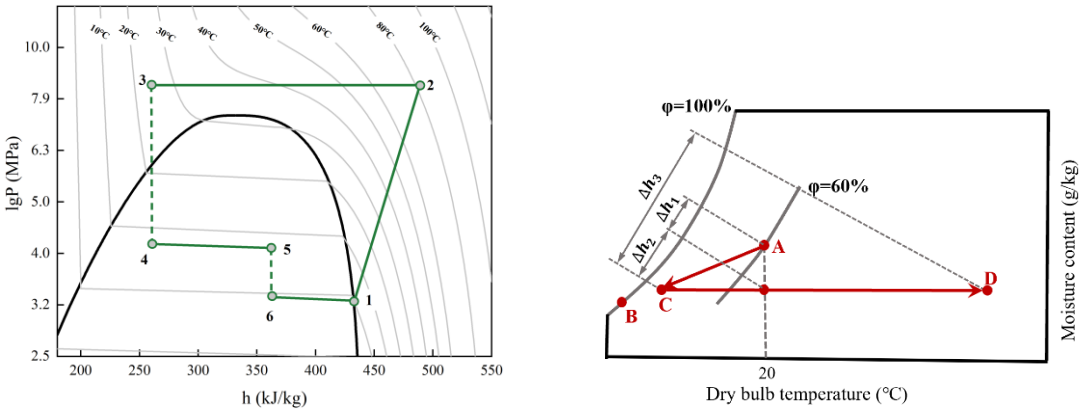

(a) The lgP-h diagram of CO_2 cycle. (b) The psychrometric chart diagram of air.

Figure 2. The schematic diagram of CO_2 cycle and indoor air treatment process.

2.2. Simulation model

GT-SUITE software is used for the modeling of the desiccant heat pump system [11] [13]. The details of the system model are shown in Table 1.

Table 1. details of the simulation model.

Equipment	Modules in GT	Dimension	Specification
Compressor	*CompPosDisp-Refrig and SpeedBound-aryRot*	Displacement: 8.2 cm^3	$\dot{m}_{CO_2} = V_{disp} \cdot \eta_v \cdot N_{com} \cdot \rho_{suc}$ $\dot{W}_{com} = \dot{m}_{CO_2} \cdot \frac{h_{dis} - h_s}{\eta_{is}} \cdot \frac{1}{\eta_e}$
Evaporators and Gascooler	*HxMaster* and *HxSlave*	Micro-channel fin-tube; Indoor Evaporator: 230 × 228 ×14 (mm) Indoor Gas Cooler: 230 × 190 × 14 Outdoor Evaporator: 660 × 515 ×16	$\dot{Q}_{HX} = \dot{m}_{CO_2}(h_{CO_2,out} - h_{CO_2,in})$ $= \dot{m}_{air} c_{p,air}(T_{air,out} - T_{air,in})$ $\dot{Q}_{HX} = \sum_{j=1}^{N} \alpha_j A_{i,j}(T_{CO_2,j} - T_{air,j})$ $\alpha_j = \left(\frac{1}{\alpha_{CO_2,j}} + \frac{A_{in,j}}{\alpha_{air,j} A_{out,j}}\right)^{-1}$
Throttle Valves	*OrificeConn*		$\dot{m}_{CO_2} = C_q \cdot A_{EEV} \cdot \sqrt{\frac{2\Delta P \cdot \rho_{EEV,in}}{k_{dp}}}$
Accumulator	*Accumulator-Refrig*	Accumulator diameter: 67 mm Accumulator height: 210 mm	
PI controller	*PID controller*		

The dehumidification rate is calculated as follows,

$$m_{vap} = m_{air} \cdot (\omega_{e,id,in} - \omega_{e,id,out}) \quad (1)$$

$$\omega_{e,id,out} = \omega_{e,id,in} + \delta \cdot (\omega_{e,wall,sat} - \omega_{e,id,in}) \quad (2)$$

$$\delta = \frac{\eta_{fin} \cdot \alpha \cdot A}{m_{air} \cdot c_{p,air}} \quad (3)$$

where, $\omega_{e,id,in}$ and $\omega_{e,id,out}$ are the inlet/outlet moist air absolute humidity in indoor evaporator, kg/kg(dry-air); δ is a heat exchange factor; $\omega_{e,wall,sat}$ is saturation absolute humidity corresponding to the wall temperature; η_{fin} is fin efficiency coefficient.

The main contributions of a dehumidifying heat pump are twofold: the first is the latent heat lost by the high humidity air during the dehumidification process ($\dot{m}_{air} \cdot \Delta h_1$), and the second is the net sensible heat of the HVAC inlet and outlet air. The desiccant heat pump coefficient of performance (DHCOP) can be used to evaluate the performance of a desiccant heat pump,

$$DHCOP = \frac{\dot{m}_{air} \cdot (\Delta h_3 - \Delta h_2)}{\dot{W}_{com}} \quad (4)$$

3. Discussion of the results

To investigate the optimal performance of the transcritical CO_2 desiccant heat pump, this study considers the effects of the environmental temperature (T_a), the indoor air mass flow rate ($\dot{m}_{air}$), the indoor evaporating pressure ($T_{e,id}$), and the compressor discharge pressure (P_{dis}) on the dehumidification rate and DHCOP. The HVAC inlet dry bulb temperature is set at 20 ℃, and the relative humidity is 60%.

Figure 3 shows the variations of DHCOP, $\dot{W}_{com}$, and $T_{gc,out}$ with respect to P_{dis} when the ambient temperature is 0 °C, $P_{e,id}$ is 38 bar, and $\dot{m}_{air}$ is 0.100 kg/s. It can be seen that there is a unique optimal P_{dis} at which DHCOP reaches its maximum value and the compressor power consumption is minimized. This is mainly due to the nearly constant load and the distribution pattern of the CO_2 isotherms in the supercritical region. The following data results are based on the optimal discharge pressure.

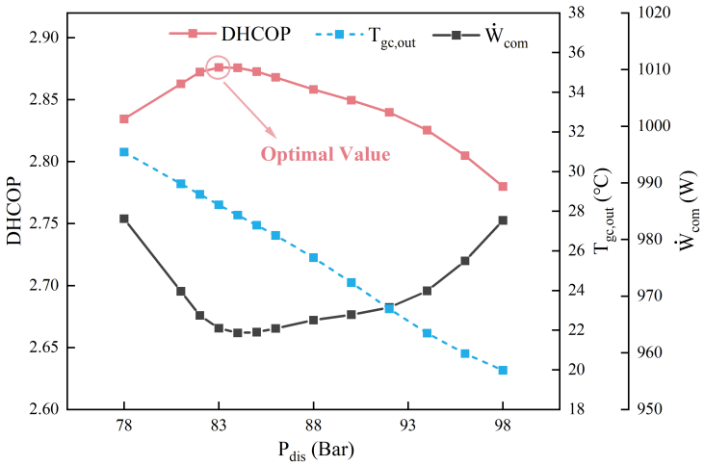

Figure 3. The variations of DHCOP, $\dot{W}_{com}$, and $T_{gc,out}$ with P_{dis}.

As shown in Table 2, the ambient temperature has little effect on the dehumidification rate. It relates to the drop in the wall temperature of the indoor evaporator pipe (due to the increase in CO_2 mass flow) is limited. However, the effect of the indoor evaporating pressure on the dehumidification rate is significant. At -10 °C, when $P_{e,id}$ decreases from 44 Bar to 36 Bar, the dehumidification rate increases by 3.56 times, reaching a maximum of 2.571×10^{-4} kg/s.

Table 2. Variation in Dehumidification Rate (10^{-4} kg/s)

$P_{e,id}$	-10 ℃	-5 ℃	0 ℃	5 ℃
36 Bar	2.571	2.614	2.650	-
38 Bar	2.151	2.172	2.212	-
40 Bar	1.703	1.722	1.761	1.777
42 Bar	1.226	1.244	1.270	1.295
44 Bar	0.722	0.737	0.761	0.766

(This study only considers the case where the indoor evaporating temperature ($T_{e,id}$) is higher than the ambient temperature. Therefore, data for $P_{e,id}$=36 Bar and 38 Bar at 5 ℃ are not available in this paper.)

Figure 4 shows the variation of the dehumidification capacity with $P_{e,id}$ as the airflow rate increases from 0.075 kg/s to 0.125 kg/s at an ambient temperature of -10 °C. It can be observed that the influence of $P_{e,id}$ on the dehumidification capacity becomes more significant as the airflow rate increases. When $\dot{m}_{air}$ is 0.075 kg/s, the dehumidification rate increases from 0.483×10^{-4} kg/s to 1.918×10^{-4} kg/s as $P_{e,id}$ decreases; while when $\dot{m}_{air}$ is 0.125 kg/s, the $\dot{m}_{vap}$ increases from 0.917×10^{-4} kg/s to 3.208×10^{-4} kg/s as $P_{e,id}$ decreases. Therefore, it can be concluded that $P_{e,id}$ and $\dot{m}_{air}$ are the main factors that affect the dehumidification rate rather than the ambient temperature.

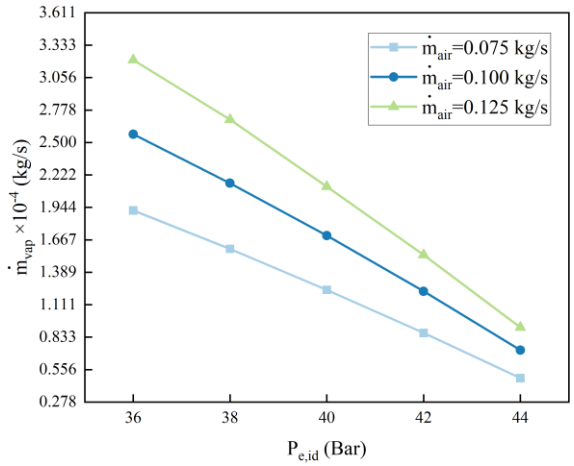

Figure 4. The variation of $\dot{m}_{vap}$ with $P_{e,id}$.

Figure 5 presents the variations of the optimal discharge pressure and the optimal HDCOP with $\dot{m}_{air}$ and $P_{e,id}$ at an ambient temperature of -10 °C. It is evident that the optimal discharge pressure shows only slight sensitivity to $P_{e,id}$, while $HDCOP_{opt}$ demonstrates a substantial decrease with increasing $P_{e,id}$. This is primarily due to $P_{e,id}$ mainly influencing the magnitude of the latent heat load, which exhibits little variation with the discharge pressure. Although an increase in $P_{e,id}$ leads to a slight rise in the gas cooler's inlet air temperature, it does not significantly impact the optimal discharge pressure. However, the latent heat load experiences a notable reduction with the increase of $P_{e,id}$, resulting in a significant decrease in $HDCOP_{opt}$. In addition, as $\dot{m}_{air}$ increases, $P_{dis,opt}$ rises due to the increased sensible heat load. Simultaneously, $HDCOP_{opt}$ also increases with the increase of $\dot{m}_{air}$, which is caused by the lower gas cooler's outlet temperature. At $\dot{m}_{air}$=0.125 kg/s and $P_{e,id}$=36 Bar, $HDCOP_{opt}$ reaches its maximum value of 2.49.

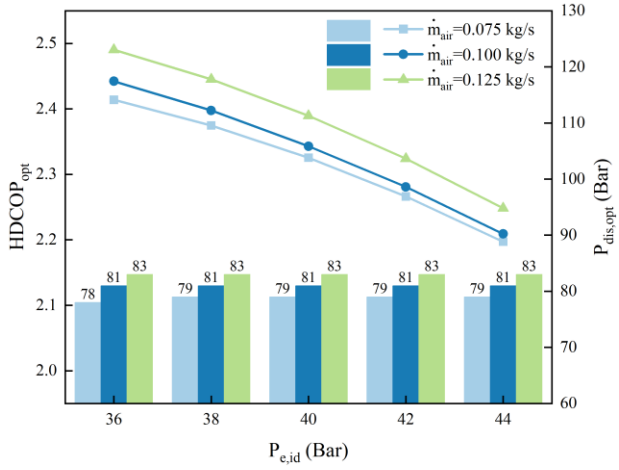

Figure 5. The variations of the $P_{dis,opt}$/$HDCOP_{opt}$ with $\dot{m}_{air}$ and $P_{e,id}$.

Figure 6 and Table 3 illustrate the variations of the $HDCOP_{opt}$ and the $P_{dis,opt}$ with respect to the T_a and $P_{e,id}$ when $\dot{m}_{air}$ is fixed at 0.100 kg/s. It can be observed that $HDCOP_{opt}$ and $P_{dis,opt}$ increase with the increase of T_a due to the elevation of the evaporation pressure. When T_a is 5 °C and $P_{e,id}$ is 40 Bar, $HDCOP_{opt}$ can reach a maximum of 3.12, indicating a potential for energy savings.

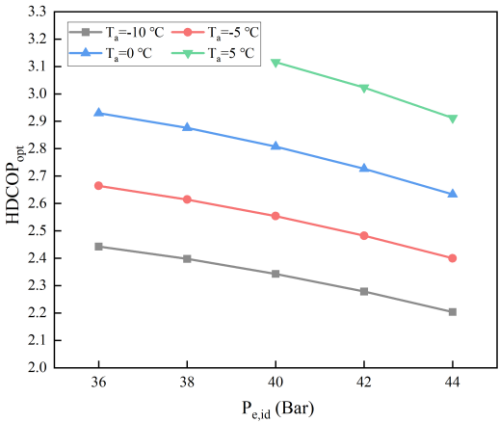

Figure 6. the variations of $HDCOP_{opt}$ in different ambient temperature.

Table 3. Variation in optimal discharge pressure (Bar)

$P_{e,id}$	-10 °C	-5 °C	0 °C	5 °C
36 Bar	81	83	84	-
38 Bar	81	83	84	-
40 Bar	81	83	84	85
42 Bar	81	83	84	85
44 Bar	81	83	84	85

4. Conclusion

This study establishes a high-fidelity model of a transcritical CO_2 desiccant heat pump to investigate the effects of environmental temperature (T_a), indoor evaporating pressure ($P_{e,id}$) and air mass flow rate ($\dot{m}_{air}$) on the desiccant heat pump coefficient of performance (HDCOP). The HDCOP not only considers the net sensible heat of the air but also takes into account the dehumidification rate.

The research reveals that a unique optimal discharge pressure exists to achieve maximum HDCOP under each operating condition. This optimal value increases with the increasing air mass flow rate and environmental temperature, but remains largely unaffected by the indoor evaporating pressure. Additionally, the dehumidification rate is minimally affected by the T_a but increases with increasing air mass flow rate and decreases with increasing indoor evaporating pressure. At $\dot{m}_{air}$=0.125 kg/s and $P_{e,id}$=36 Bar, the dehumidification rate can reach 3.208×10^{-4} kg/s .

It is noteworthy that HDCOP increases with the elevation of environmental temperature and air mass flow rate but decreases with increasing indoor evaporating pressure. Despite the challenging operating conditions at -10 °C, the HDCOP of the transcritical CO_2 desiccant heat pump can still exceed 2.1, while reaching 3.12 at a moderate condition of T_a=5 °C. The transcritical CO_2 heat pump desiccant system demonstrates significant energy-saving potential.

Appendices

Nomenclature

A	Heat exchange area, (m^2)	η_e	Compressor motor efficiency
$c_{p,air}$	Air specific heat capacity, (kJ/(kg·K))	η_{is}	Compressor isentropic efficiency
DHCOP	Desiccant heat pump coefficient of performance	η_V	The ratio of the theoretical volume of the expander to the compressor
EV	Electric vehicle	ρ	Density, (kg/m^3)
HVAC	Heating, Ventilation, and Air Conditioning	ω	Moist air absolute humidity, (kg/kg(dry-air))
h	Enthalpy, (kJ/kg)	φ	Relative humidity
k			
$\dot{m}_{air}$	Air mass flow rate, (kg/s)	**Subscripts**	
$\dot{m}_{vap}$	Dehumidification rate, (kg/s)	a	Ambient
N_{com}	Speed of compressor, (RPM)	air	Air
P	Pressure, (bar)	dis	Discharge of Compressor
PTC	Positive Temperature Coefficient	e	Evaporator
$\dot{Q}$	Quantity of heat, (W)	EEV	Electronic expansion valve
T	Temperature, (℃)	gc	Gas cooler
V_{disp}	Displacement, (m^3)	HX	Heat exchanger
$\dot{W}_{com}$	Power consumption, (W)	id	Indoor
		suc	Suction of Compressor
Greek symbols			
α	Surface heat transfer coefficient, ($W/(m^2·K)$)		

References

[1] Christian T, Adolfo P and Arnaud M 2010 Cost and CO_2 aspects of future vehicle options in Europe under new energy policy scenarios *Energy Policy* **38(11)** 7142-7151.
[2] Lohse-Busch H, Duoba M, Rask E, Stutenberg K, Gowri V, Slezak L and Anderson D 2013 Ambient temperature (20°f, 72°f and 95°f) impact on fuel and energy consumption for several conventional vehicles, hybrid and plug-in hybrid electric vehicles and battery electric vehicle *SAE Technical Paper* **01** 1462.
[3] Jeffers M A, Chaney L and Rugh J P 2016 Climate control load reduction strategies for electric drive vehicles in cold weather *SAE Int. J. Passeng. Cars - Mech. Syst.* **9(1)** 75-82.
[4] Yang D, Huo Y, Zhang Q, Xie J and Yang Z 2022 Recent advances on air heating system of cabin for pure electric vehicles: A review *Heliyon* **8(10)** e11032.
[5] Zhang Z, Li W, Zhang C and Chen J 2017 Climate control loads prediction of electric vehicles *Appl. Therm. Eng.* **110** 1183-1188.
[6] Lee S, Chung Y, Jeong and Kim M S 2022 Investigation on the performance enhancement of electric vehicle heat pump system with air-to-air regenerative heat exchanger in cold condition *Sustainable Energy Technol. Assess.* **50** 101791.
[7] Zhang Z, Wang D, Zhang C and Chen J 2018 Electric vehicle range extension strategies based on improved AC system in cold climate – A review *Int. J. Refrig.* **88** 141-150.
[8] Li Z, Hashimoto K, Hasegawa H and Saikawa M 2018 Performance analysis of a heat pump

system with integrated desiccant for electric vehicles *Int. J. Refrig.* **86** 154-162.
[9] Wu J, Zhou G and Wang M 2020 A comprehensive assessment of refrigerants for cabin heating and cooling on electric vehicles *Appl. Therm. Eng.* **174(25)** 115258.
[10] Dong J, Wang Y, Jia S, Zhang X and Huang L 2021 Experimental study of R744 heat pump system for electric vehicle application *Appl. Therm. Eng.* **183 Part 1 25** 116191.
[11] Wang H, Cao F, Jia F, Song Y and Yin X 2023 Potential assessment of transcritical CO_2 secondary loop heat pump for electric vehicles. *Appl. Therm. Eng.* **224** 119921.
[12] Wang D, Yu B, Hu J, Chen L, Shi J and Chen J 2018 Heating performance characteristics of CO_2 heat pump system for electrical vehicle in a cold climate *Int. J. Refrig.* **85** 27-41.
[13] Wang H, Song Y, Qiao Y, Li S and Cao F 2022 Rational assessment and selection of air source heat pump system operating with CO_2 and R407C for electric bus *Renew. Energy* **182** 86-101.

Acknowledgments
The authors are grateful to the foundation for Innovative Research Groups of the National Natural Science Foundation of China (No.51721004) (F.Cao) and China Scholarship Council (No. 202206280214) (H. Wang).